Critical state in a circular two-dimensional superconductor and magnetization of thin $Nd_{1.85}Ce_{0.15}CuO_{4-\delta}$ and $YBa_2Cu_3O_{7-\delta}$ films in a transverse field

A. V. Kuznetsov, A. A. Ivanov, and D. V. Eremenko
Department of Quantum Electronics, Moscow Engineering Physics Institute, Kashirskoe shosse 31, 115409, Moscow, Russia

V. N. Trofimov
Laboratory of Nuclear Problems, Joint Institute for Nuclear Research, 141980, Dubna, Moscow region, Russia
(Received 10 February 1995)

Precise measurements of the magnetization of circular epitaxial $Nd_{1.85}Ce_{0.15}CuO_{4-\delta}$ and $YBa_2Cu_3O_{7-\delta}$ films in a transverse magnetic field are performed and analyzed within the framework of the recently presented critical state model (CSM) in the two-dimensional superconductor. Restrictions on the reliability of the model are considered. It has been found that the original CSM, based on Bean's limitation on the critical current density J_c=const, describes well the temperature and field dependences of the film magnetization in a low field (until the full disappearance of the flux-free region in the film) under the condition $B^* \gg \mu_0 d J_c \ln(\sqrt{Rd}/\lambda)$, where B^* is the characteristic field of the critical current drop in a strong field, λ is the penetration depth, d is the thickness, and R is the radius of the film, respectively. In the strong field an exponential or power suppression of the critical current is observed and the model under question is extended to this region. The problem of a lower critical field related to thin films is also discussed. The paramagnetic response demonstrated by all our films in field-cooled measurements, which has much in common with the Wohlleben effect, was investigated and the conclusion was drawn that this artifact is caused by the temperature-dependent stray field of the magnetometer parts.

I. INTRODUCTION

A thin film with $d<\lambda$, where d is the thickness and λ is the penetration depth, in a transversely applied magnetic field B_a represents a two-dimensional (2D) superconductor whose behavior is different from that of a bulk specimen.[1-3] The magnetic field penetrates into the film in the form of vortices,[4-6] which have the radius of the core much larger than the coherence length ξ and nonexponential decay of the associated field and supercurrent at a characteristic length $\Lambda=2\lambda^2/d$. In thermodynamic equilibrium in the applied field $B_a \gg B_{c1f}$, where B_{c1f} is the lower critical field of the film, vortices generate a uniform triangular lattice,[2] while in the case of nonzero pinning the film is divided into two regions, as illustrated in Fig. 1. The inner part, $0<r<a$, where a is the flux-front position, demonstrates a no-vortex Meissner state. In the external region, $a<r<R$, where R is the radius of the film, a mixed state is realized and the vortices are pinned. The Maxwell equation $\mathbf{J}=\mu_0^{-1}\mathrm{rot}\mathbf{B}$, where $\mathbf{B}=\mathbf{B}_a+\mathbf{B}_d$ and $\mathbf{B}_d$ is the demagnetization field, is valid everywhere, though with a different physical meaning of the related quantities in these two parts. In the mixed state, according to the critical state model (CSM), $\mathbf{J}$ and $\mathbf{B}$ are macroscopic quantities, obtained upon averaging of the respective microscopic ones over some region containing few vortices, and in addition the equation $J=J_c[B(r)]$ is postulated. In the Meissner part $\mathbf{J}$ and $\mathbf{B}$ are the usual local quantities. Therefore, the current distribution over the whole circular film can be found from the equation $\mathbf{J}=\mu_0^{-1}e_\varphi(\partial B_r/\partial z-\partial B_z/\partial r)$ with the additional conditions $B_z=0$ when $a>r>0$ and $J=J_c$ when $R>r>a$. Note that only $B_z(r)$ is determined by the local density of vortices, and therefore the critical current is not proportional to the gradient of flux density, as is postulated in Bean's original CSM,[7] developed for a bulk specimen with zero demagnetization factor. The first term in rot$\mathbf{B}$, attributed to the distortion of the field by the film, is different from zero everywhere except the center of the film. The second term, which is equal to the radial gradient of the flux density, exists only in the mixed state region. As was noted in Ref. 8, in a thin film $\partial B_r/\partial z$

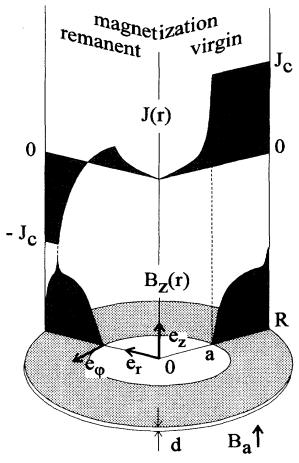

FIG. 1. Space patterns of current and $B_z(r)$ in a circular-shaped film after increase (right) and subsequent decrease to zero (left) of the applied field, e_z,e_r, and e_φ are the unit vectors in the cylinder frame of reference, d is the thickness of the film, R is its radius, and a is the flux-front position. The Meissner state region is $r<a$; the mixed state region is $a<r<R$.

exceeds $\partial B_z/\partial r$ in a weak field.

The equation under consideration is nonlinear and nonlocal, because the demagnetization field $\mathbf{B}_d$ depends on the induced current at every point of the film. The solution for a stationary and alternating applied field has been found within Bean's approximation $J_c=\text{const}$ for a circular film[9–11] and a long rectangular strip.[12–14] In Ref. 15 an induced electric field arising at high frequencies of the applied magnetic field is taken into account to describe the dynamic behavior of the film.

When the whole circular film is in the Meissner state the current distribution can be written[9,16]

$$\mu_0 dJ = 2B_r = (4/\pi)B_a r/\sqrt{R^2-r^2}\ .$$

In the mixed state both components of the field $B_r=\mu_0 dJ/2$ and $B_z=B_a+B_{dz}$ are different from zero with a distribution found in Refs. 9 and 10 and depicted in Fig. 1. The flux distribution can be measured directly by means of a Hall sensor or through the magneto-optic effect and, hence, $B_z(r)$ can be restored, as was done, for example, in Ref. 8 (see also references in Refs. 13 and 14). Any developed CSM in a 2D superconductor, which may give current and field patterns, and consequently such an integral quantity as the magnetic moment, can be verified upon comparison with experimental magnetization curves versus temperature and field. That is the purpose of the present paper with respect to the CSM originally developed in Ref. 9 and extended in Refs. 10 and 11. According to Ref. 9, the virgin magnetic moment of the circular film in the mixed state can be written as

$$\mathbf{M} = -\frac{D^3}{3\mu_0}\mathbf{B}_a S(x)\ ,$$
$$S(x) = \frac{1}{2x}\left[\arccos\frac{1}{\cosh x} + \frac{\sinh|x|}{\cosh^2 x}\right]\ , \tag{1}$$

where $x=B_a/B_c$, and $B_c=\mu_0 dJ_c/2$ is a characteristic field. According to Ref. 10, the remanent moment is

$$\mathbf{M}_{\text{rem}} = \frac{D^3}{3\mu_0}\mathbf{B}_a[S(x/2)-S(x)]\ . \tag{2}$$

The respective patterns of the current and flux are presented in Fig. 1 too.

Our measurements[17] confirm formulas (1) and (2) for the field $B_a \lesssim 4B_c$ very well. However, the critical current and the magnetic moment are suppressed by a strong field, and the CSM under consideration, which is based on Bean's approximation $J_c=\text{const}$, is no longer valid. To overcome this restriction we discuss the behavior of the magnetic moment in a weak and a strong applied field. The peculiarities related to samples of a hard superconductor with a high demagnetization factor are discussed, including an artifact imitating the Wohlleben effect (paramagnetic Meissner effect). Section II describes the experimental procedure. Section III contains a comparison of the measured and calculated magnetization versus field and temperature. In Sec. IV limitations on the original CSM are discussed as well as the behavior of the film beyond this model. The final part represents a summary.

II. MATERIALS AND METHODS

Epitaxial films of $Nd_{1.85}Ce_{0.15}CuO_{4-\delta}$ and $YBa_2Cu_3O_{7-\delta}$ were laser ablated onto circular substrates cut from $SrTiO_3(100)$ and yttrium stabilized zirconium oxide (YSZ) (100) plates. The details of the fabrication of $Nd_{1.85}Ce_{0.15}CuO_{4-\delta}$ and $YBa_2Cu_3O_{7-\delta}$ films by means of the pulsed-laser deposition technique have been reported earlier.[18] According to x-ray diffraction measurements, the films were (001) oriented with disorientation less than 0.5°, which was determined by disorientation of the substrate. The thickness of the films was measured with an interference microscope with the accuracy of 20 nm.

The external field was applied perpendicular to the plane of the film. In this configuration, a large demagnetization factor and strong pinning, demonstrated by the films, put severe requirements on the magnitude, uniformity, and reproducibility of the "zero" field in the magnetometer, which strongly affects the remanent magnetization in a weak field. This is the reason why we have updated our superconducting quantum interference device (SQUID) susceptometer[19] to be able to start measurements in a very weak field. The low-temperature part of the insert after modernization is shown in Fig. 2. The magnetic field produced by a copper solenoid is trapped with a niobium tube which is coaxial to the pickup coils and the channel in which the probe with the sample moves. The external fields are screened with two cast lead screens with spherical bottoms. The ambient "zero" field of the magnetometer measured with the probe lead cylinder is 1 μT, irrespective of the applied field up to 7 mT at least. This upper upper limit on the measuring field in a low-field mode of operation arises from the maximum power dissipated in the solenoid, which does not overheat the trapping tube above critical temperature.

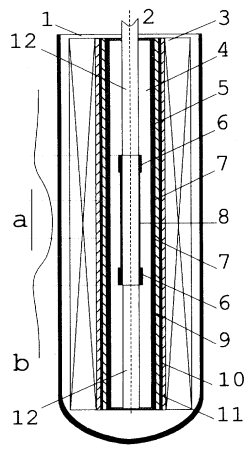

FIG. 2. A scheme of the insertable part of the magnetometer. 1, lead screen; 2, channel for sample probe; 3, copper solenoid; 4, vacuum insulator for copper oven; 5, copper frame for pickup coils, 6, heaters of oven; 7, pickup coils of flux transformer; 8, copper oven; 9, niobium field-trapping tube; 10, copper heater; 11, thermal insulation; 12, thin-walled stainless-steel thermal impedance between the oven and liquid helium; *a*, scanning length for measuring; *b* stray field pattern along axis.

The measurements in a strong-field mode, up to 1 T, have been performed with a superconducting magnet.

The temperature was varied in the range 4.2–300 K discretely or continuously at a rate of 20–50 mK/s and was measured with an accuracy of 50 and 100 mK below and above 30 K, respectively. The temperature dependence of magnetization was measured upon continuous temperature change with the sample fixed in one of the pickup coils, after the standard procedure of zero-field cooling (ZFC), field cooling (FC), or warming in the remanent state (rem) had been carried out. A background response obtained under the same procedure, but without the sample, was then subtracted to derive the magnetization of the film proper versus temperature. The background temperature curve, which we mainly attributed to the temperature-dependent magnetization of the thin-walled stainless-steel tubes whose ends are located 25 mm off the pickup coils, was highly reproducible.

Four samples of each above-mentioned high-temperature superconductor (HTSC) were investigated with quite similar behavior observed. The NdCeCuO samples are labeled as S1–S4 and the YBaCuO ones as Y1–Y 4. The results discussed below are related to the $Nd_{1.85}Ce_{0.15}CuO_{4-\delta}$ sample S1 with diameter $D=2.42$ mm and thickness $d=150$ nm, if not stated otherwise. The difference between $Nd_{1.85}Ce_{0.15}CuO_{4-\delta}$ and $YBa_2Cu_3O_{7-\delta}$ samples is considered in the last part of the next section.

III. RESULTS

A. The temperature curves

The curves $M_{ZFC}(T)$, $M_{FC}(T)$, and $M_{rem}(T)$ are presented in Fig. 3 for two values of the applied field, 7.8 and 371 μT. Obviously, M_{FC} is much smaller than M_{ZFC} and M_{rem}, and thus the flux expulsion is strongly suppressed. At temperatures below T_c the derivative dM/dT is the same for all three quantities, as if some additive $M_0(T)$ independent of what is measured exists. If we subtract this term, then $M_{FC}(T)=0$ and $M_{ZFC}(T)=-M_{rem}(T)$ at all applied fields. This means that both M_{ZFC} and M_{rem} indicate the same critical temperature and are irreversible at all temperatures within the accuracy of our measurements.

According to Eq. (1), the temperature dependence of M_{ZFC} is determined by the temperature dependence of the critical current density J_c. As soon as the latter is measured, $M_{ZFC}(T)$ can be calculated. Within Bean's approximation, both field-saturated M_{ZFC} and M_{rem} are equal to $M_s=(\pi/24)D^3dJ_c$. We have derived $J_c(T)$ from the field-saturated $M_{rem}(T)$ and fitted it to the function

$$J_c(T)=J_c(0)\times(1-t^2)^{2.7}/(1+t^2)^{2.4},$$

where $t=T/T_c$, the measured critical temperature $T_c=20.7$ K, and $J_c(0)=2.44\times10^{10}$ A m^{-2}, which is calculated using the above-mentioned dimensions of the sample. The results are shown in Fig. 4. The measured and calculated curves $M_{ZFC}(T)$ are compared in Figs. 5 and 3(a). We want to stress that no free fitting parameters have been used. As is seen, Bean's approximation is applicable in the whole temperature range and the small deviation near T_c is probably caused by the $J_c(T)$ fit error in this region.

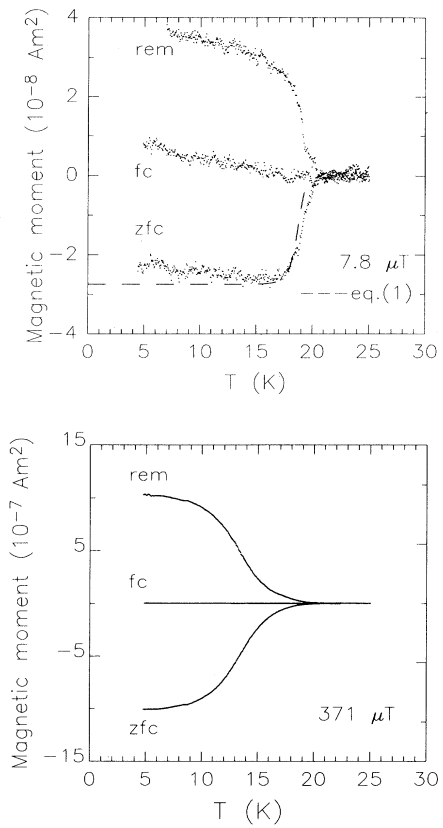

FIG. 3. The temperature curves $M_{ZFC}(T)$, $M_{FC}(T)$, and $M_{rem}(T)$ of $Nd_{1.85}Ce_{0.15}CuO_{4-\delta}$ film. The dashed line is calculated from (1) using the experimental $J_c(T)$ fitted to the function shown in Fig. 4.

It is interesting to discuss the anomalous sign of M_{FC} which corresponds to paramagnetic behavior. This was a common feature of all the films, both $Nd_{1.85}Ce_{0.15}CuO_{4-\delta}$ (Fig. 6) and $YBa_2Cu_3O_{7-\delta}$ (Fig. 7), more clearly pro-

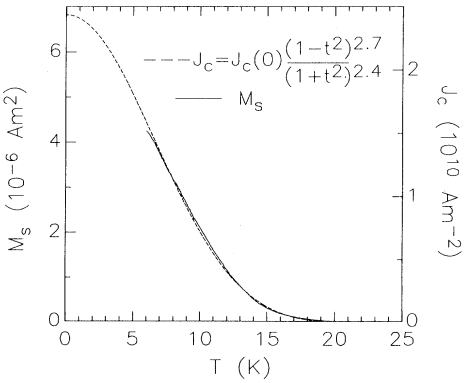

FIG. 4. Experimental saturated remanent moment and the corresponding critical current density of the $Nd_{1.85}Ce_{0.15}CuO_{4-\delta}$ film (solid line) and a fit (dashed line) with $t=T/T_c$, $T_c=20.7$ K (measured), and adjustable free parameter $J_c(0)=2.44\times10^{10}$ A m^{-2}.

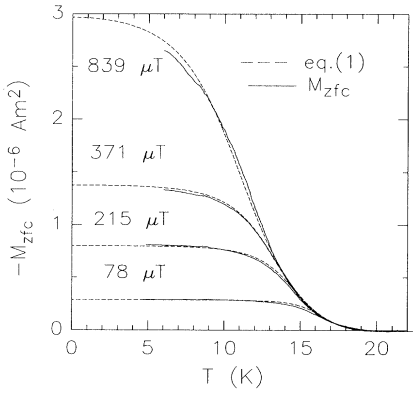

FIG. 5. $M_{ZFC}(T)$ of the $Nd_{1.85}Ce_{0.15}$ $CuO_{4-\delta}$ films corresponding to the measurement (solid line) and calculation from (1) (dashed line).

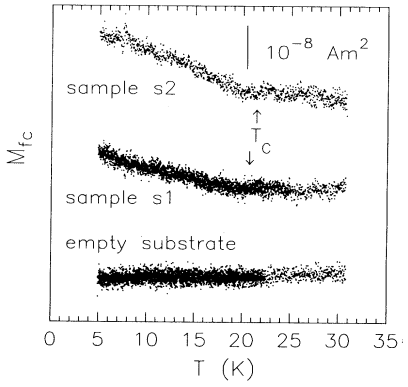

FIG. 6. $M_{FC}(T)$ plots of two $Nd_{1.85}Ce_{0.15}CuO_{4-\delta}$ films and an empty substrate recorded under the same procedure. Each curve is measured for five values of the applied field: 7000, 839, 371, 78, and 7.8 μT. The arrows mark the critical temperature values.

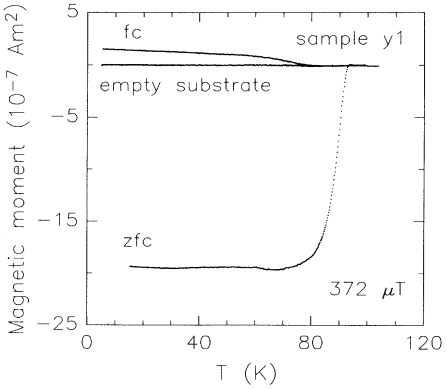

FIG. 7. $M_{ZFC}(T)$ and $M_{FC}(T)$ plots of the $YBa_2Cu_3O_{7-\delta}$ film and an empty substrate.

nounced for the latter. As is seen from Fig. 6, where the curves $M_{FC}(T)$ for two $Nd_{1.85}Ce_{0.15}CuO_{4-\delta}$ samples and an empty substrate are displayed, the "paramagnetic" response is not related to the substrate. We summarize here the following features of the observed phenomenon.

(a) It was demonstrated by all investigated films.

(b) The temperature variation of M_{ZFC}, M_{FC}, and M_{rem} below T_c is the same.

(c) M_{FC} is independent of the applied field. Each curve in Fig. 6 is a superposition of many with the applied field covering three orders of magnitude, from 7.8 μT to 7 mT.

Taking all this into account we attributed the "paramagnetic" M_{FC} to the temperature dependence of the stray field in the magnetometer which adds to the applied field. This addition arises from the temperature-dependent remanent magnetization of the ends of the thin-walled stainless tubes which form a channel for the sample probe and serve as a thermal impedance between the copper oven and liquid helium. The possible axial pattern of the stray field is shown in Fig. 2. We have evaluated that the observed variation of M_{FC} upon cooling from 100 to 4.2 K corresponds to a stray field variation equal to a few μT, which looks quite realistic.

B. Field-induced isotherms

The isotherms $M(B_a)$ and $M_{rem}(B_a)$ were measured by increasing the applied field to B_a and then decreasing it back to zero with increasing magnitude of B_a. Because of the stray field, M_{ZFC} at applied field $B_a=0$ is different from zero, $M_{ZFC}(T,0)=M_0(T)\neq 0$. This initial magnetic moment slightly disturbs $M(B_a)$, but strongly affects the low-field behavior of $M_{rem}(B_a)$. The value of $M_0(T)$ was taken into account by comparison of the measured and calculated quantities. To calculate M and M_{rem} according to formulas (1) and (2), the measured $J_c(T)$ (Fig. 4) was used as a parameter.

The isotherms $M(B_a)$ shown in Fig. 8 demonstrate good agreement between the measured and calculated

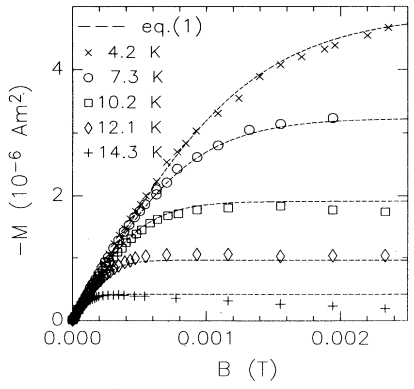

FIG. 8. $M(B_a)$ isotherms of the $Nd_{1.85}Ce_{0.15}CuO_{4-\delta}$ film, measured (points) and calculated from Eq. (1) (dashed line). B_c values 1.8, 1.2, 0.64, 0.37, and 0.16 mT corresponding to $T=4.5$, 7.3, 10.2, 12.1, and 14.3 K, respectively, are determined through $J_c(T)$ and the thickness of the film.

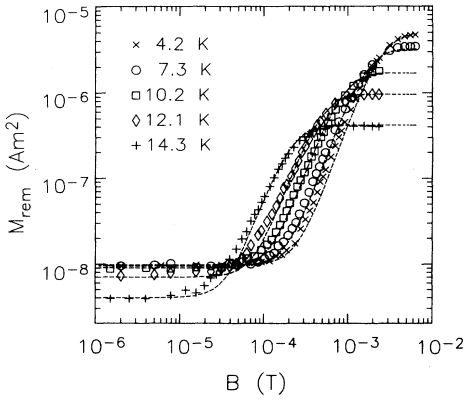

FIG. 9. $M_{rem}(B_a)$ isotherms of the $Nd_{1.85}Ce_{0.15}CuO_{4-\delta}$ film. The dashed curves are plotted according to the expression $M^*_{rem}(B_a)=M_0(T)+M_{rem}(B_a)$, where $M_{rem}(B_a)$ is calculated according to Eq. (2) and $M_0 \approx M_{FC}(T)$ (see Fig. 5, sample S1).

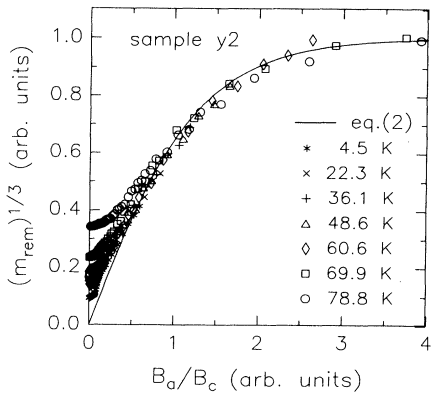

FIG. 10. Reduced $M_{rem}(B_a)$ isotherms of the $YBa_2Cu_3O_{7-\delta}$ film vs the reduced field $x=B_a/B_c(T)$. The solid curve is calculated as $\sqrt[3]{m_{rem}}$, where $m_{rem}(x)=(4/\pi)[S(x/2)-S(x)]x$. Points are experimental values reduced as the third root of $(12\mu_0/\pi D^3)M_{rem}/B_c$ and $B_c(T)$ is an adjustable parameter of the fit.

curves for all temperatures except close to T_c. The interpretation of the magnetization curve is quite simple. In a weak field $B_a \ll B_c$ only a narrow fringe at the edge of the film is in a mixed state; hence the current distribution is nearly the same as that in the Meissner state and the moment is proportional to the applied field with the temperature-independent slope $D^3/3\mu_0$.[9,16] As the field is increased, the flux front moves to the center of the sample and the rate of the moment growth drops until M saturates at $B_a \simeq 2B_c$. The following decrease in magnetization in strong field $B_a \gg B_c$ shows that the field dependence of the critical current should be taken into account. Our results for the $Nd_{1.85}Ce_{0.15}CuO_{4-\delta}$ film behavior in a strong field were presented earlier.[16]

The isotherms $M_{rem}(B_a)$ are shown in Fig. 9 in a double-logarithmic plot. The experimental data are well described with the relation $M^*_{rem}(B_a)=M_0(T)+M_{rem}(B_a)$, where $M_{rem}(B_a)$ is calculated according to Eq. (2), though some deviation is clearly seen. In a very weak field remanence is nearly constant because $M_0 \gg M_{rem}$. In an intermediate region $B_a \lesssim B_c$ remanence increases by a power law with the exponent slightly decreasing with increasing temperature. At $T=4.5$ K the exponent $n=2.3$. On the other hand, the expansion of (2) in terms of x shows that at $x<1$ the exponent should be equal to 3, irrespective of the temperature. The greater the ratio M_0/M_s is, the more the measured $M_{rem}(B_a)$ deviates from the behavior predicted by Eq. (2). We assume therefore that the discrepancy concerning M_{rem} between the model and the experiment may be caused by the nonzero moment M_0. The remanence saturates in the field $B_a \simeq 4B_c$. The saturated values of M_{rem} coincide with the values obtained in the temperature measurements of $M_s(T)$ depicted in Fig. 4.

C. $YBa_2Cu_3O_{7-\delta}$ films

The magnetic properties of the $YBa_2Cu_3O_{7-\delta}$ films are quantitatively similar to those of $Nd_{1.85}Ce_{0.15}CuO_{4-\delta}$, but the critical current density is one order of magnitude higher. At low temperature the characteristic field B_c is equal to a few tens of mT; therefore, to obtain the complete experimental data in order to compare the theory and experiment, as described above for $Nd_{1.85}Ce_{0.15}CuO_{4-\delta}$, the upper limit of the applied field should not be less than 0.1–0.3 T. This program regarding $YBa_2Cu_3O_{7-\delta}$ films could be performed with our magnetometer by two separate measurements, either in a low-field mode with the copper solenoid, or in a strong-field mode with the superconducting magnet. Only the first part has been done. Hence saturated mode magnetization was not achieved for most of the temperature range below T_c, and $J_c(T)$ was not derived independently. We have assumed that the original CSM is valid for the $YBa_2Cu_3O_{7-\delta}$ films too, and fitted the measured low-field isotherms for the remanent moment by (2), using J_c as a free parameter. This procedure yielded $J_c(T)$. To make this, according to a low-field expansion $M_{rem} \sim (B_a/B_c)^3$ of (2), the third root of the measured reduced remanence isotherm $(12\mu_0/\pi D^3)M_{rem}/B_c$ versus the reduced field $x=B_a/B_c$ was fitted by the corresponding reduced quantity $\sqrt[3]{m_{rem}}$, calculated from Eq. (2), where

$$m_{rem}(x)=M_{rem}/M_s=(4/\pi)[S(x/2)-S(x)]x \ .$$

The result is represented in Fig. 10. The visible deviation of the experimental data form the calculated curve in the weak-field region is caused by the nonzero initial moment $M_0(T)$ as discussed above. The fitting parameter $B_c(T)$ gave then the critical current $J_c(T)=2B_c(T)/\mu_0 d$, which is shown in Fig. 11. The temperature dependence obtained for sample Y2 is well fitted to the function

$$J_c(T)=J_c(0)\times(1-T/T_c)^{1.4} \ ,$$

where T_c is measured to be 89 K and $J_c(0)=1.46\times10^{11}$ A m^{-2}, as was calculated for $d=140$ nm.

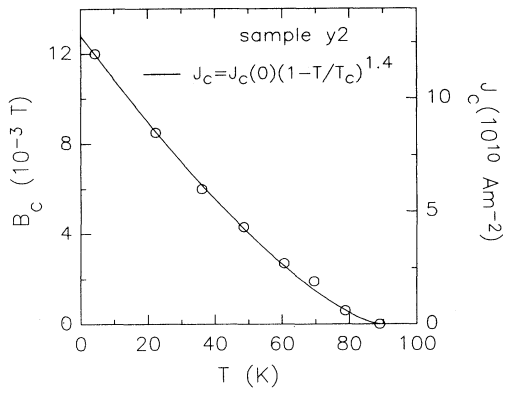

FIG. 11. Temperature dependences of the characteristic field $B_c(T)$ and critical current density $J_c(T)$ of the $YBa_2Cu_3O_{7-\delta}$ film determined by fitting the low-field measured data to those calculated from the 2D CSM under consideration. The solid line is a fit $J_c(T)=J_c(0)\times(1-T/T_c)^{1.4}$, where $J_c(0)=1.46\times10^{11}$ A m^{-2} and measured $T_c=89$ K.

IV. DISCUSSION

As shown in the previous sections, the CSM in a 2D circular superconductor[9,10] describes well the penetration of the flux into $Nd_{1.85}Ce_{0.15}CuO_{4-\delta}$ films. A great advantage of Eqs. (1) and (2) is the absence of free fitting parameters. They include only the dimensions of the film, its critical current density, and the value of the applied field. It seems very important to consider the limitations on the validity of the solutions found in Refs. 9–14, which arise from the initial assumptions and the properties of 2D superconductors.

We assume the film to be thin enough to neglect the current variation along the thickness, i.e., $d<\lambda$, where $\lambda=\lambda_{ab}$ when the c axis is normal to the plane of the HTSC film. In a 2D superconductor the characteristic length of change for the vortex current and field is $\Lambda=2\lambda^2/d$, which can be macroscopically large near T_c or for very thin films. Any CSM introduces field and current averaged over some region containing a number of vortices. This puts a lower limit on the dimension of the film, $D\gg\Lambda$, and excludes temperatures near T_c. The range of exclusion depends on $D/\Lambda(T)$.

It is well known that the structures of the vortex in 2D and bulk superconductors are different. In a film the radius of the core is $r_c=\sqrt[3]{12\Lambda\xi^2}$,[2] the current drops as $1/r^2$ when $r>\Lambda$, and the interaction potential decreases as $1/r$, in contrast to a bulk superconductor, where it decreases exponentially at $r\gg\lambda$. The principal difference between film and bulk samples is the existence in the film of the weakly screened long-range interaction between vortices, induced by overlapping of their fields in the surrounding space.[1–3] Strong interaction of vortices should generate a high sensitivity of the critical current to the local flux density. The problem of the field dependence of the critical current in HTSC films is discussed below. First we shall consider the behavior in a low field and evaluate the field range of existence of the Meissner state.

A. Low magnetic field

The lower critical field B_{c1f} of the film is small compared with the characteristic fields which determine the flux penetration. For this reason, B_{c1f} is assumed to be zero in the framework of the CSM under discussion. We think that the measurement of B_{c1f} is a separate important problem[20] and here only the relation between B_{c1f} and the dimensions of the sample will be considered.

In general, when the intermediate or mixed state occurs in a superconductor the value of the applied field B_p can be found by the minimization of its free energy. This is the penetration field. To calculate analytically the field-dependent free energy of a sample with an arbitrary shape seems impossible. For this reason it is commonly recognized that the Meissner state begins to disappear when the maximum field at the surface $B_{\tau m}$ achieves the lower critical field B_{c1} for a type-II superconductor, or the thermodynamic critical field B_c for a type-I superconductor. In both cases the critical field corresponding to a bulk specimen with zero demagnetization factor is implied. It is clear that a more correct consideration should include the dependence of the thermodynamic critical field on the thickness of the sample.[4,5] An additional assumption involves the equality in the field and current patterns of the real sample and an inscribed ellipsoid. For the latter the relation $B_{\tau m}(B_a)$ can be found analytically and then the penetration field can be derived as a solution of the equation $B_{\tau m}(B_p)=B_{c1}$. For a disk-shaped sample, for instance, this approximation gives $B_{\tau m}=(2/\pi)(D/d)B_a$ and $B_p=(\pi/2)(d/D)B_{c1}$. The penetration field calculated within this approximation is close to the measured one for samples with a low demagnetization factor, but much lower for the samples with a high demagnetization factor.[21,22] As was noted in Refs. 16, 20, and 23, this discrepancy can be explained if one takes into account the relation between the density of the Meissner current, and hence B_τ, and the curvature of the superconductor surface k. The curvature $k_e\simeq 2D/d^2$, and hence the enhancement of the applied field, at the equator of the inscribed ellipsoid is larger than that for the sample with thickness d, for which the rough estimate of the edge curvature is $k_s\simeq 2/d$. Therefore, a more accurate approximation may be based on the equality of the local fields at the edge of the sample and the ellipsoid of approximation. The small axis a of the latter can then be found from the equation $2/d\simeq 2D/a^2$. This model gives $B_p\simeq(2/\pi)B_{c1}\sqrt{d/D}$,[16] while the experimental data for bulk lead disks and thick films[21,22] are well fitted to the formula $B_p=(4/\pi)B_{c1}\sqrt{d/D}$.

The above is valid only when $d\gg\lambda$. For a thin film no simple way to find $B_{\tau m}(B_a)$ is seen so far, either analytically or experimentally. Besides this difficulty, B_{c1} attributed to a bulk superconductor should be replaced by the critical field B_{c1f} attributed to a 2D superconductor. The difference between these quantities is generated by the difference in the magnetic moment m and energy per unit length U_c of the vortex in bulk and 2D superconductors. In Ref. 3 the Ginzburg-Landau equation was solved for a thin circular film in a transverse field and the lower critical field was found to be $B_{c1f}=\Phi_0U_c/D\Lambda m$, where Φ_0 is

the flux quantum and U_c and m are dimensionless quantities. In the limit $D \gg \Lambda$, the latter are equal to $U_c = \ln\sqrt{\Lambda/r_c}$ and $m = \pi/2$,[3] and the lower critical field can then be written as

$$B_{c1f} = \frac{4}{3}\frac{d}{D}B_{c1}\left[1+\frac{\ln(\lambda/d\sqrt{3})}{\ln\kappa}\right], \quad (3)$$

where $B_{c1} = (\Phi_0/4\pi\lambda^2)\ln\kappa$ is the lower critical field of the bulk superconductor. A more accurate calculation[3] shows that B_{c1f} is slightly smaller, because m obeys logarithmic growth with increasing ratio D/Λ and goes over the limit $\pi/2$.

Taking the published data for $Nd_{1.85}Ce_{0.15}CuO_{4-\delta}$,[24] $\lambda_{ab}(0) \simeq 150$ nm, $\xi_{ab}(0) \simeq 8$ nm, and for $YBa_2Cu_3O_{7-\delta}$,[25,26] $\lambda_{ab}(0) \simeq 140$ nm, $\xi_{ab}(0) \simeq 1.7$ nm, and the typical dimensions of our films, $D \simeq 2.5$ mm, $d \simeq 150$ nm, we obtain $B_{c1f} \simeq 1.5$ μT and $B_{c1f} \simeq 2.5$ μT, respectively. These values are the lower limits for the field, corresponding to arising of the first vortex; B_p may be higher due to the geometrical barrier.[27,28]

Lets now consider how the finite value of B_{c1f}, which is of the same order as the "zero" field in our magnetometer, affects the magnetization curves. The expansion of (1) in terms of $x = B_a/B_c \ll 1$ shows that in a weak field the magnetic moment in the mixed state is the same as in the Meissner state, $M = -(D^3/3\mu_0)B_a$. Consequently, the nonzero value of B_{c1f} does not influence the curve $M(B_a)$, but remanence will arise only when $B_a > B_{c1f}$ and will increase as $M_{\rm rem} \sim (B_a - B_{c1f})^3$, as follows from expansion of (2).

The weak-field behavior of the remanence $M_{\rm rem}(B_a)$ is complicated in our case by the existence of the nonzero initial moment M_0 (see Fig. 9), which also presented itself as anomalous FC magnetization.

For a hard superconductor the reversible and irreversible flux expulsion should be taken into account.[29] The former can be neglected for our samples because we have not observed reversible magnetization at all temperatures. Similarly, the narrow temperature region near T_c, where it should be, was beyond our temperature resolution, while at other temperatures the applied field was small compared with the field of irreversibility. Extreme narrowness of the reversible magnetization region for weak fields has been observed in a $Nd_{2-x}Ce_xCuO_{4-\delta}$ single crystal[30] as well. Upon cooling in the field, the flux in the presence of pinning can vary within the edge fringe with the characteristic flux-trapping width $L(T)$, which can be evaluated as[29,31]

$$L(T) = \frac{p}{\mu_0}\frac{\partial B_{c1}/\partial T}{\partial J_c/\partial T} = \frac{pd}{2}\frac{\partial B_{c1}/\partial T}{\partial B_c/\partial T}, \quad (4)$$

where p is a numerical factor less than unity. In the inner part of the sample the flux is frozen. Evidently, L is of the order of d, and therefore we can neglect the flux expulsion in all magnetization processes. The flux in the film is frozen uniformly under the superconductive transition and $M_{\rm FC}$ should be equal to zero. When the stray field in the magnetometer B_s is temperature dependent, then an additional moment $M_0 \simeq -(D^3/3\mu_0)B_s$ occurs which adds to $M_{\rm ZFC}$, $M_{\rm rem}$, or $M_{\rm FC}$ [see Fig. 3(a)]. Its amplitude does not depend on the applied field until B_s is independent of B_a. This is what we have observed and illustrated in Fig. 6.

It is easy to see that $M_0(T)$ has much in common in behavior with the Wohlleben effect (WE) (or paramagnetic Meissner effect), investigated in Refs. 32–39. In particular, the most striking feature is that $M_{\rm FC}$ is independent of the applied field as well.[34,35] The WE has been observed in powders,[35,36] ceramics,[32–35] single crystals[37,38] of Bi-based HTSC's, and even in a niobium disk.[39] It was found for textured powder, a single crystal, and a niobium disk that the WE exists in a transverse field and disappears in a longitudinal one. Decreasing the powder size strongly depresses the WE.[35,36] The evidence of the demagnetization factor involvement makes the WE explanation via Josephson π links[40] very questionable. In any case, when hard superconductor samples with a high demagnetization factor are studied the probability of an artifact similar to what we have observed should be taken into account.

To gain insight into the mechanism of flux penetration near B_{c1f}, we intend to decrease the "zero" field in our magnetometer down to 100 nT, at least.

B. Strong magnetic field

Because the pinning potential in HTSC's is small, the critical current is strongly depressed by the magnetic field. To describe this, exponential $J_c(T,B) = J_c(T)\exp(-B/B^*)$ (Ref. 41) or power-law $J_c(T,B) = J_c(T)/(1+B/B^*)^n$, $0 < n < 1$,[42] dependences are most frequently used. Note that the characteristic field B^* also depends on temperature. The CSM in a 2D superconductor was developed within Bean's approximation. The solution of the critical-state equation with a field-dependent critical current is not obtained yet, but numerical methods to derive field and current patterns have been proposed.[14,43] We shall calculate the magnetic moment in a strong field, when the whole circular film with thickness $d < \lambda$ and diameter D is in a mixed state and for both types of critical current versus field dependence. Reversible magnetization of the film is neglected.

In the cylinder reference frame the disturbed field and induced current can be written as

$$\mathbf{B} = \mathbf{e}_r B_{dr}(r) + \mathbf{e}_z[B_a + B_{dz}(r)]$$

and $I(r) = dJ_c F(r)$, where B_{dz} and B_{dr} are the axial and radial components of the current-induced demagnetization field, J_c is the critical current density in the zero field, and the function $F = F(B(r))$ determines the field dependence of the critical current and can vary from 0 to 1. On the surface of the film we have $B_{dr} \ll B_{dz}$; therefore $B \simeq B_a + B_{dz}(r)$ and

$$B_{dz}(r) = \frac{B_c}{\pi}\int_0^R F(\rho)\left[\frac{K(m)}{\rho+r}+\frac{E(m)}{\rho-r}\right]d\rho, \quad m = \frac{4\rho r}{(\rho+r)^2}, \quad (5)$$

where $B_c=\mu_0 dJ_c/2$ and E and K are the complete elliptic integrals of the first and second kind, respectively. When $r=R$, the integral diverges logarithmically at an upper limit. However, as was mentioned above, within the CSM it is impossible to consider the field and current variation in a fringe with width less than Λ at the edge of the film. Therefore one can formally take the upper limit in (5) as $r_e \simeq R-\Lambda$ instead of R. Clearly, the largest value of $B_{dz}(r)$ is reached when the critical current does not depend on the field, i.e., $F(r)=1$. Then we can estimate[44]

$$B_{dz}(r) \leq B_{dz}(r_e) \simeq B_c \ln(R/\Lambda) .$$

Let us first consider an exponentially suppressed current in the limit $B^* \gg B_c \ln(R/\Lambda)$. Then

$$F(r)=\exp(-B/B^*) \simeq [1-B_{dz}(r)/B^*]\exp(-B_a/B^*) .$$

This yields a magnetic moment

$$M=\pi \int_0^R I(r) r^2 dr$$

$$=\frac{\pi}{3} R^3 dJ_c e^{-B_a/B^*} \left[1-\frac{3}{R^3 B^*}\int_0^R B_{dz}(r) r^2 dr\right] . \quad (6)$$

Substituting $B_{dz}(r)$ from (5) and bearing in mind that $F(r)<1$, one can estimate the integral at $F(r)=1$:

$$\frac{3B_c}{\pi B^* R^3}\int_0^R \int_0^R \left[\frac{K}{\rho+r}+\frac{E}{\rho-r}\right] r^2 d\rho\, dr$$

$$=\frac{B_c}{\pi B^*}(2G-1) \approx 0.265 \frac{B_c}{B^*} , \quad (7)$$

where

$$G=\sum_{k=0}^{\infty} \frac{(-1)^k}{(2k+1)^2}=0.9159...$$

is Kathalan's constant. Finally, the moment can be written as

$$M=\frac{\pi}{24} D^3 dJ_c e^{-B_a/B^*}=M_s e^{-B_a/B^*} . \quad (8)$$

In the case of power-dependent current, one can write

$$F(r)=\{1+[B_a+B_{dz}(r)]/B^*\}^{-n} .$$

It is easy to show that at $B^* \gg B_a$ and $B^* \gg B_c \ln(R/\Lambda)$ the moment is estimated as

$$M \simeq M_s\{1-n[B_a+B_c(2G-1)/\pi]/B^*\} \simeq M_s ,$$

and at $B_a \gg B_c \ln(R/\Lambda)$ the moment is

$$M=\frac{M_s}{(1+B_a/B^*)^n} . \quad (9)$$

At $B_a \gg B^*$ the moment decreases as $(B_a)^{-n}$. This was observed in $YBa_2Cu_3O_{7-\delta}$ ceramics;[45] one could expect the same in films, but as a matter of fact magnetization of the $YBa_2Cu_3O_{7-\delta}$ and $Bi_2Sr_2CaCu_2O_8$ films demonstrates exponential field suppression.[46]

In the $Nd_{1.85}Ce_{0.15}CuO_{4-\delta}$ films we have observed an exponential drop of the moment in a strong field. The

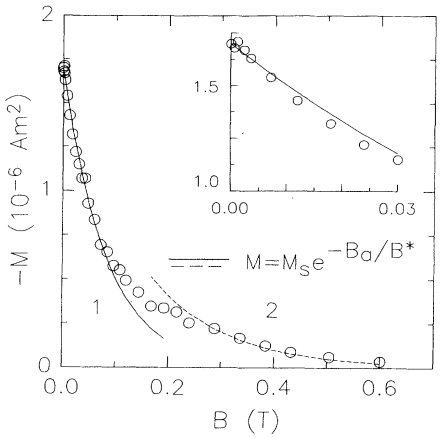

FIG. 12. Wide-range field magnetization of the $Nd_{1.85}Ce_{0.15}CuO_{4-\delta}$ film sample S3 at 4.2 K. The solid and dashed curves are calculated from the relation $M=M_s \exp(-B_a/B^*)$ with $B^*=80$ and 140 mT, respectively. The inset shows the low-field magnetization.

magnetization curve for sample S3, displayed in Fig. 12, represents two exponential regions and a weakly pronounced peak effect[47] at $B_a \simeq 0.2$ T. The field B^* was found by fitting to (8) with J_c measured in the low-field range. The values corresponding to the two regions are $B^*=80$ mT and $B^*=140$ mT. The same field dependence of magnetization was observed in single-crystal $L_{2-x}Ce_xCuO_{4-\delta}$ (L =Nd, Pr),[30] and was attributed to the pinning centers generated by oxygen vacancies. However, the current here is less affected by the field as compared with films. For example, $B^*=0.4$ T at 4.2 K in a $Nd_{1.85}Ce_{0.15}CuO_{4-\delta}$ single crystal.

In the present report we describe the magnetization which relaxed within $t \simeq 100$ s, the characteristic time interval of measurement. The largest density of unrelaxed critical current in the $Nd_{1.85}Ce_{0.15}CuO_{4-\delta}$ films is $J_c(0)=5\times10^{10}$ A m^{-2},[48] i.e., 5% of the depairing current $J_0 \simeq 1\times10^{12}$ A m^{-2}.[30] Therefore the pinning is relatively strong.

The value of the applied field corresponding to disappearance of the Meissner state and defined in the literature as the field of complete penetration B_{CP} can be found from the equation $a \simeq \Lambda$, where a was earlier defined as the flux-front position and is equal to $a=R/\cosh(B_a/B_c)$.[9] From this it follows that

$$B_{CP} \simeq B_c \ln(D/\Lambda)=\mu_0 J_c d \ln(\sqrt{Rd}/\lambda)$$

which is of the same order as the maximum value of the demagnetization field $B_{dz}(r_e) \simeq B_c \ln(R/\Lambda)$. Because $\lambda_{ab}<250$ nm in HTSC's for samples with $D>0.1$ mm and $d>100$ nm the complete penetration field ($B_{CP} \gtrsim 4.4B_c$) exceeds the saturation fields for the virgin moment ($B_a \simeq 2B_c$) and remanent moment ($B_a \simeq 4B_c$) as well. If the characteristic field B^* is much higher than B_{CP}, the penetration of flux can be described within Bean's approximation according to Eqs. (1) and (2) until the full disappearance of the Meissner state. As can easi-

ly be seen, this condition is feasible for our films. For example, sample S3 (see Fig. 12) obeys $B_{CP} \simeq 4$ mT and $B^* \geq 80$ mT at 4.2 K. Nevertheless, in some $Nd_{1.85}Ce_{0.15}CuO_{4-\delta}$ films with relatively low critical current, it was inhibited by the applied field at high temperatures $T > 0.7T_c$ before the saturation of the remanence occurs. Consequently, to consider the magnetization of such specimens, the field dependence of the critical current should be taken into account for all applied field.

V. SUMMARY

(1) We have found an excellent agreement between virgin and remanent magnetization in the field and temperature domains, calculated within the modern CSM in a circular-shaped film and measured in $Nd_{1.85}Ce_{0.15}CuO_{4-\delta}$ films. No free parameters have been used. The temperature-dependent critical current which is needed to compare the theory and experiment was measured through saturated remanence at different temperatures and the feasibility of this procedure was then justified.

(2) The critical current versus temperature in a $YBa_2Cu_3O_{7-\delta}$ film was derived on the assumption that the CSM in question is valid for this film too. The fitting of the calculated magnetization to the one measured in the low-field range when saturated remanence was not achieved for most temperatures was performed with $J_c(T)$ as a free parameter.

(3) The limitations on the validity of the 2D CSM have been considered. We concluded that a clear picture arises from introducing a hierarchy of characteristic fields: B_p, the penetration field which is more than or equal to the lower critical field of a film B_{c1f}; $B_{CP} \simeq \mu_0 J_c d \ln(\sqrt{Rd}/\lambda)$, the complete penetration field of a film; and B^*, the characteristic field of the critical current suppression by the field. Then the condition for the application of the 2D CSM can be expressed as $B^* \gg B_{CP} \gtrsim B_a > B_p$, where B_a is an applied field.

(4) For the field region $B_a > B_{CP}$ the formula for film magnetization was extended to the case of exponential or power-dependent critical current versus field.

(5) We studied the "paramagnetic" FC response, observed in all the films being investigated, which had much in common with the Wohlleben effect, and concluded that it was caused by a temperature-dependent stray field of the magnetometer parts.

ACKNOWLEDGMENTS

We would like to thank Dr. A. Sinchenko for helpful discussions and Dr. S. Galkin and Dr. O. Churkin for assistance in the measurements. The work was supported by ISF Grant No. MG2000 and carried out within the framework of the Scientific Programme "Universities of Russia."

[1] J. Pearl, in *Proceedings of the Ninth Inernational Conference on Low Temperature Physics,* edited by J. G. Daunt, D. V. Edwards, F. G. Milford, and M. Yagub (Plenum, New York, 1965), Part A, p. 566; Appl. Phys. Lett. **5**, 65 (1964).
[2] A. L. Fetter and P. C. Hohenberg, Phys. Rev. **159**, 330 (1967).
[3] A. Fetter, Phys. Rev. B **22**, 1200 (1980).
[4] M. Tinkham, Phys. Rev. **129**, 2413 (1963).
[5] G. D. Gody and R. E. Miller, Phys. Rev. Lett. **16**, 697 (1966).
[6] The existence of vortices was explained (Ref. 4) in thin films of type-I superconductors, the magnetization curves of which are similar to those of hard superconductors (Ref. 5).
[7] C. P. Bean, Phys. Rev. Lett. **8**, 250 (1962).
[8] H. Theuss, A. Forkl, and H. Kronmüller, Physica C **190**, 345 (1992).
[9] P. N. Mikheenko and Yu. E. Kuzovlev, Physica C **204**, 229 (1993).
[10] J. Zhu, J. Mester, J. Lockhart, and J. Turneaure, Physica C **212**, 216 (1993).
[11] John R. Clem and Alvaro Sanchez, Phys. Rev. B **50**, 9355 (1994).
[12] E. H. Brandt, M. Indenbom, and A. Forkl, Europhys. Lett. **22**, 735 (1993).
[13] E. H. Brandt and M. Indenbom, Phys. Rev. B **48**, 12 893 (1993).
[14] E. Zeldov, John R. Clem, M. McElfresh, and M. Darwin, Phys. Rev. B **49**, 9802 (1994).
[15] E. H. Brandt, Phys. Rev. B **49**, 9204 (1994); **50**, 4034 (1994).
[16] V. N. Trofimov, A. V. Kuznetsov, P. V. Lepeshkin, K. A. Bolshinskov, A. A. Ivanov, and A. A. Mikhailov, Physica C **183**, 135 (1991).
[17] A. Kuznetsov, V. Trofimov, A. Ivanov, and A. Sinchenko, in Proceedings of the 4th International Conference on Materials & Mechanisms of Superconductivity of High-Temperature Superconductors [Physica C **235–240**, 2851 (1994)].
[18] A. A. Ivanov, S. G. Galkin, A. V. Kuznetsov, and A. P. Menushenkov, Physica C **180**, 69 (1991).
[19] V. N. Trofimov, Cryogenics **32**, 513 (1992).
[20] V. Trofimov and A. Kuznetsov, in Proceedings of the 4th International Conference on Materials & Mechanisms of Superconductivity of High-Temperature Superconductors (Ref. 17), p. 2853.
[21] R. H. Huebener, R. T. Kampwirth, and J. R. Clem, J. Low Temp. Phys. **6**, 275 (1972).
[22] M. N. Kunchur and S. J. Poon, Phys. Rev. B **43**, 2916 (1991).
[23] V. N. Trofimov, A. V. Kuznetsov, A. A. Sinchenko, K. A. Bolshinskov, and A. A. Ivanov, Physica B **194–196**, 2327 (1994).
[24] L. Fábrega, J. Fontcuberta, B. Martìnez, and S. Piñol, Phys. Rev. B **50**, 3256 (1994).
[25] A. Schilling, F. Hulliger, and H. R. Ott, Physica C **168**, 272 (1990).
[26] Z. Hao, J. R. Clem, M. W. McElfresh, L. Civale, A. P. Malozemoff, and F. Holtzberg, Phys. Rev. B **43**, 2844 (1991).
[27] M. V. Indenbom, H. Kronmüller, T. W. Li, P. H. Kes, and A. A. Menovsky, Physica C **222**, 203 (1994).
[28] E. Zeldov, A. I. Larkin, M. Konczykowski, B. Khaykovich,

D. Majer, V. B. Geshkenbein, and V. M. Vinokur, in Proceedings of the 4th International Conference on Materials & Mechanisms of Superconductivity of High-Temperature Superconductors (Ref. 17), p. 2761.

[29]J. R. Clem and Z. Hao, Phys. Rev. B **48**, 13 774 (1993).

[30]L. Fàbrega, J. Fontcuberta, and S. Piñol, Physica C **224**, 99 (1994).

[31]In Ref. 29 a superconductor with zero demagnetization factor was treated; nevertheless, to estimate the order of $L(T)$ magnitude we use the appropriate expression from this paper substituting in it the fields calculated with demagnetization included.

[32]W. Braunisch, N. Knauf, V. Kataev, S. Neuhansen, A. Grütz, A. Kock, B. Roden, D. Khomskii, and D. Wohlleben, Phys. Rev. Lett. **68**, 1908 (1992).

[33]B. Schliepe, M. Stindtmann, I. Nikolic, and K. Barberchke, Phys. Rev. B **47**, 8331 (1993).

[34]Ch. Heinzel, Th. Theilig, and P. Ziemann, Phys. Rev. B **48**, 3445 (1993).

[35]W. Braunisch, N. Knauf, G. Bauer, A. Kock, A. Becker, B. Freitag, A. Grütz, V. Kataev, S. Neuhansen, B. Roden, D. Khomskii, and D. Wohlleben, Phys. Rev. B **48**, 4030 (1993).

[36]D. Khomskii, in Proceedings of the 4th International Conference on Materials & Mechanisms of Superconductivity of High-Temperature Superconductors [Physica C **235–240**, 293 (1994)].

[37]A. K. Grover, N. Goyal, F. Iga, K. Ino, N. Aoki, Y. Yamaguchi, and Y. Nishihara, in Proceedings of the 4th International Conference on Materials & Mechanisms of Superconductivity of High-Temperature Superconductors (Ref. 17), p. 3281.

[38]A. K. Pradhan, S. B. Roy, P. Chaddah, C. Chen, and B. M. Wanklyn, in Proceedings of the 4th International Conference on Materials & Mechanisms of Superconductivity of High-Temperature Superconductors (Ref. 17), p. 1947.

[39]M. S. M. Minhaj, D. J. Thompson, L. E. Wenger, and J. T. Chen, in Proceedings of the 4th International Conference on Materials & Mechanisms of Superconductivity of High-Temperature Superconductors (Ref. 17), p. 2519.

[40]L. N. Bulaevskii, V. V. Kuzii, A. A. Sobyanin, Pis'ma Zh. Eksp. Teor. Fiz. **25**, 317 (1977) [JETP Lett. **25**, 290 (1977)].

[41]G. R. Kumar and P. Chaddah, Phys. Rev. B **39**, 4704 (1989).

[42]M. Xu, D. Shi, and R. F. Fox, Phys. Rev. B **42**, 10 773 (1990).

[43]Yu. A. Fedorov, V. G. Fleisher, and M. G. Semenchenko, Physica C **217**, 63 (1993).

[44]This is an upper estimation of the demagnetization field value. In reality, it does not exceed B_a anywhere, except the film edge (Refs. 8 and 9), where its maximum value is limited by $B_c \ln(R/\Lambda)$, as follows from the critical current suppression by the field.

[45]W. J. Yeh, Z. Q. Yu, S. Labroo, and J. Y. Park, Physica C **194**, 141 (1992).

[46]T. Nojima and T. Fujita, Physica C **178**, 140 (1991).

[47]K. Kadowaki and T. Mochiku, Physica C **195**, 127 (1992).

[48]The results on the study of remanence relaxation in $Nd_{1.85}Ce_{0.15}CuO_{4-\delta}$ thin films will be published elsewhere.